CHEMICAL ENGINEERING TRANSACTIONS

VOL. 88, 2021

A publication of AIDIC
The Italian Association of Chemical Engineering
Online at www.cetjournal.it

Guest Editors: Petar S. Varbanov, Yee Van Fan, Jiří J. Klemeš

ISBN 978-88-95608-86-0; **ISSN** 2283-9216

DOI: 10.3303/CET2188066

An Experimental Investigation to Determine the Effect of Tube Material on the Tubeside Heat Transfer Performance of the Enhanced 1EHT Three Dimensional Heat Transfer Tube

David John Kukulka[a,*], Wei Li[b], Rick Smith[c]

[a] State University of New York College at Buffalo, 1300 Elmwood Avenue, Buffalo, New York, 14222 USA,
[b] Department of Energy Engineering, Zhejiang University, 866 Yuhangtang Road, Hangzhou 310027, PR China
[c] Vipertex, 658 Ohio Street, Buffalo New York. USA
kukulkdj@buffalostate.edu

Condensation heat transfer characteristics were experimentally investigated over a wide range of operating conditions in order to determine the heat transfer performance inside horizontal, smooth and enhanced heat transfer tubes; using R410A in tubes produced of copper and stainless steel. Experimental data was verified and results were compared to the performance measured in a smooth tube. Results indicate that the condensation heat transfer coefficient (HTC) enhancement ratio is in the range from 1.15 to 2.05 for the 1EHT tube and for the HX tube it ranged from 1.18 to 1.69. Smooth tube heat transfer performance was slightly affected by the thermal conductivity of the tube; however, larger enhancements are found in the enhanced tubes.
Heat transfer coefficients increase with an increase of mass velocities. When the mass flux increases, the liquid flow becomes more turbulent and the liquid film becomes thinner; this reduces the thermal resistance and enhances the heat transfer. Heat transfer performance for low mass velocities rise slowly, showing only a small difference in magnitude. Performance increase is larger at high mass flux rates than that those found at low mass fluxes. The influence of thermal conductivity on the condensation heat transfer of the enhanced horizontal tubes was discussed. Better heat transfer performance occurs in tubes produced of a higher thermal conductivity material (copper) or in tubes with a smaller diameter.

1. Introduction

Heat transfer enhancement methods are efficient ways to conserve energy and various aspects have been previously investigated. Surface enhancement is a heat transfer technique commonly employed in various industries (i.e. air conditioning, aerospace, refrigeration, etc.) to enhance system performance. Condensation heat transfer characteristics were experimentally investigated to determine the heat transfer performance inside enhanced heat transfer tubes and smooth tubes; with tubes produced using different tube materials (copper and stainless steel); using R410A; for a variety of operating conditions.
Li et al. (2020) evaluated heat transfer performance of several stainless-steel enhanced surface tubes with the smooth, herringbone, helix micro-grooves, herringbone-dimple, and hydrophobic surfaces. Gu et al. (2020) conducted experiments to study the condensation heat transfer characteristics of moist air outside three-dimensional (3D), finned tubes. Zhang et al. (2018) experimentally studied the condensing heat transfer characteristics (when using R410A) inside smooth and micro-fin tubes. Zhao et al. (2017) studied the influence of surface structure and thermal conductivity on the condensation HTC inside enhanced 2D and 3D finned tubes made of iron cupronickel and aluminium brass. Ji et al. (2014) discuss the material/conductivity differences of enhanced tube materials and relate thermal conductivity differences to fin efficiency. Ali et al. (2013) reported experimental data for condensation when using ethylene glycol and R-113 in three identical pairs of pin-fin tubes made of copper, brass and bronze. Tang et al. (2020) observed and analyzed the flow patterns during condensation (using R410A) inside three-dimensional enhanced tubes made of stainless steel and copper. Their results show that the transition between annular flow and intermittent flow was shifted to a lower vapor quality

Paper Received: 18 June 2021; Revised: 1 September 2021; Accepted: 11 October 2021
Please cite this article as: Kukulka D.J., Li W., Smith R., 2021, An Experimental Investigation to Determine the Effect of Tube Material on the Tubeside Heat Transfer Performance of the Enhanced 1EHT Three Dimensional Heat Transfer Tube, Chemical Engineering Transactions, 88, 397-402 DOI:10.3303/CET2188066

for the enhanced tubes. Li et al. (2017), they evaluated the condensation heat transfer characteristics (using R22 and R410A) in micro-fin tubes and compared the performance to smooth horizontal tubes, with outer diameters of 5 mm and 9.52 mm. Kukulka et al. (2014) evaluated the inside condensation and evaporation heat transfer of R410A, R22 and R32 that took place in a 12.7 mm horizontal cooper tube with low mass fluxes; they found that tubeside evaporation and condensation HTC enhancement of the 1EHT tube is approximately 2 times greater than smooth tubes. Kukulka et al. (2019) conducted an experimental investigation to explore the heat transfer coefficient and the frictional pressure drop during condensation and evaporation using 1EHT tubes over a limited range of conditions. As can be seen there is little published data regarding enhanced EHT tubes and this apparent lack of information provides the motivation for this study. Little published data exist on: comparative analysis of various enhanced dimensional tubes; evaluation of tube material; heat transfer performance evaluation; heat transfer performance of different sized enhanced tubes. The work of Tang et al. (2020) and Li et al. (2017) have been extended in this study and includes: a smooth tube, 2D helix micro-fin tube and a 3D 1EHT tube; with different tube thermal conductivities and diameters. An investigation of the condensation heat transfer characteristics was performed using different tube thermal conductivities, tube diameters, and surface structures.

2. Experimental Details

Figure 1 is the experimental apparatus used in this study. Table 1 provides the main parameters of the tubes tested; pictures of the enhanced surfaces are presented in Figure 2.

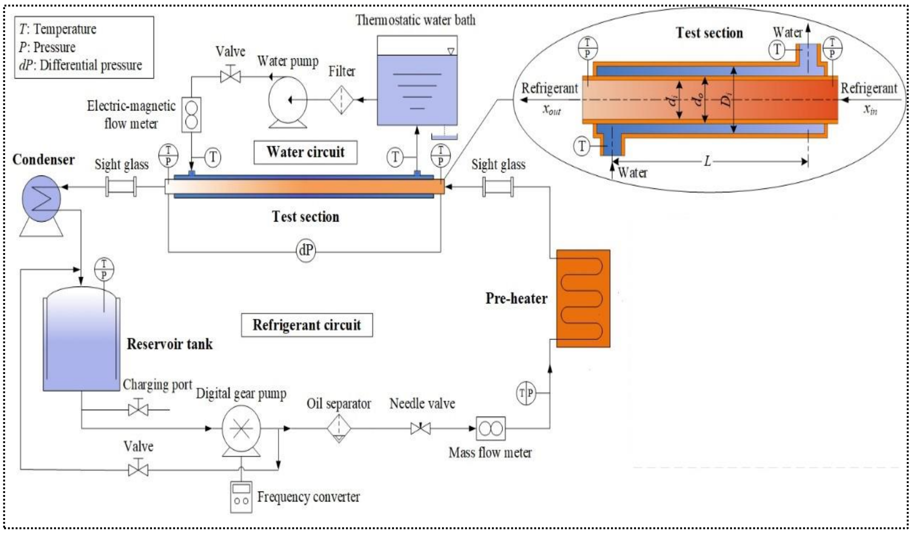

Figure 1 Schematic diagram of the experimental setup

Table 1: Geometric parameters of the tested tubes

Parameter	Smooth tube	1EHT tube	HX tube
Material	Cu/SS	Cu/SS	Cu/SS
Outer diameter (mm)	9.52/12.7	9.52/12.7	9.52/12.7
Thickness (mm)	0.61	0.61	0.61
Length (mm)	2	2	2
Dimple/fin height (mm)	-	0.19/1.71	0.25
Dimple/fin width (mm)	-	0.35/1.34	0.31
Dimple/fin pitch (mm)	-	4	0.8
Helix angle (°)	-	60	21
Surface Area enhancement ratio (1)	1	1.44	1.34

Deionized water is the working medium used in the constant temperature water bath in the experiment section; industrial alcohol is used to run at a lower temperature in the supercooling section. As shown in Figure 1, the test section is a typical horizontal, tube-in-tube heat exchanger with a heated length of 2.0 m. Tubes evaluated are utilized as the inner tube, a copper tube with an outer diameter of 17.0 mm is utilized as the outer tube.

Experimental conditions to investigate the effects of tube diameter and material include: saturation temperature of 45 ºC; mass flux values in the range of 75 to 400 kg m^{-2} s^{-1}; with an inlet vapor quality of 0.8 and outlet vapor quality of 0.2. Maximum relative error of the HTC is calculated to be ± 11.32 %; Table 2 presents the maximum relative errors of the measurement and calculation parameters.

(a) 1EHT tube

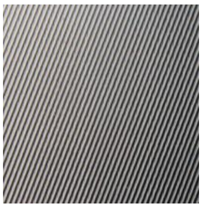

(b) HX tube

Figure 2: Pictures of enhanced surfaces: (a) 1EHT (b) HX

Table 2: Maximum relative errors of measurement and calculation parameters

Measurement Parameters	**Uncertainty**
Diameter (mm)	± 0.05
Length (mm)	± 0.2
Temperature (K)	± 0.05
Pressure (range: 0 - 40 bar)	± 0.2 % of full scale
Differential pressure (range: 0 - 100 kPa)	± 0.05 % of reading
Water flow rate (range: 0 - 12 L min^{-1})	± 0.35 % of reading
Refrigerant flow rate (range: 0 - 60 kg h^{-1})	± 0.2 % of reading

Calculation Parameters	**Uncertainty**
Mass flux (kg $m^{-2}s^{-1}$)	± 3.25 %
Heat flux (W m^{-2})	± 4.71 %
Vapor quality	± 6.30 %
Heat transfer coefficient (W m^{-2} k^{-1})	± 11.32 %

3. Results

Data were evaluated using the necessary fluid properties from Lemmon et al. (2010). Heat transfer, Q_{te}, in the test section is determined using the heat flux of the annular waterside, $Q_{w,te}$, as shown in Eq(1) :

$$Q_{te} = Q_{w,te} = c_w m_{w,te}\left(t_{w,te,out} - t_{w,te,in}\right) \tag{1}$$

where c_w is the specific heat capacity of water; $m_{w,te}$, water mass flux in the test section; $t_{w,te,out}$ and $t_{w,te,in}$ are the outlet and inlet water temperature in the test section. In order to perform a heat balance analysis, the heat flux of the refrigerant, $Q_{re,te}$, is calculated using:

$$Q_{re,te} = m_{re,te}\left(x_{in} i_{v,in} + (1 - x_{in}) i_{l,in} - [(1 - x_{out}) i_{l,out} + x_{out} i_{v,out}]\right) \tag{2}$$

where $m_{re,te}$ is the refrigerant mass flux in the test section; $i_{v,in}$ and $i_{v,out}$ are the gaseous enthalpy of the refrigerant in the test section inlet and outlet; $i_{l,in}$ and $i_{l,out}$ are the liquid enthalpy of refrigerant in the test section inlet and outlet. Inlet and outlet vapor quality of the refrigerant, x_{in} and x_{out} are determined from:

$$x_{in} = \frac{i_{in} - i_s}{i_v} \tag{3}$$

$$x_{out} = \frac{i_{out} - i_s}{i_v} \tag{4}$$

where i_{in} is the enthalpy of the refrigerant at the inlet of the test section; i_{out} is the enthalpy of the refrigerant at the outlet; i_s, the enthalpy of the saturated liquid; and i_v, the vaporization enthalpy of the refrigerant at the saturation temperature. Enthalpy at the outlet of the preheat exchanger can be computed from the enthalpy at the inlet of the preheat exchanger, $i_{pr,in}$; heat flux in the preheat exchanger, Q_{pr}; and the refrigerant mass flux in the preheat exchanger, m_{re}, as follows:

$$i_{in} = i_{pr,in} + \frac{Q_{pr}}{m_{re}} \tag{5}$$

Similarly, the enthalpy of the refrigerant at the outlet of the test section is calculated from the enthalpy at the test section inlet, $i_{te,in}$; heat flux in the test section, Q_{te}; and the refrigerant mass flux, m_{re}, as follows:

$$i_{out} = i_{in} + \frac{Q_{te}}{m_{re}} \tag{6}$$

The heat transfer coefficient is computed in Eq(7):

$$h_{re,te,i} = \frac{1}{A_i\left[\frac{LMTD}{Q_{te}} - \frac{1}{h_{w,te,o}A_o} - \frac{ln(d_o/d_i)}{2\pi L \cdot k}\right]} \tag{7}$$

where A_i and A_o are the heat transfer areas of the refrigerant side and waterside; $h_{w,te,o}$, waterside heat transfer coefficient; L , tube length; k, thermal conductivity of the tested tube; d_i , nominal inner diameter of the tube evaluated; d_o , outer diameter of the evaluated tube and LMTD, the logarithmic mean temperature difference.

Effects of tube parameters (wall thermal conductivity and tube inner diameter -ID) on the inside tube HTC is discussed. Results showing the condensation HTCs inside copper and stainless-steel tubes with a 12.7-mm OD; as a function of mass flux are compared in Figure 3. Differences in enhanced tube performance are the result of differences in tube material thermal conductivity. Smooth tube copper HTCs are slightly higher than those found in the SS smooth tubes; while the HTCs inside the copper enhanced tubes are significantly higher than enhanced SS tubes.

Effects of tube material thermal conductivity on the inside condensation heat transfer of enhanced tubes was determined from the experimental results. Performance differences observed in tubes produced from different tube material conductivity is explained because of temperature differences produced by the fin efficiency of the enhanced surface. The structure of the enhanced surfaces produces different temperature gradients for different thermal conductivity values; the actual temperature of the heat transfer surface is not the same as the fin root temperature. For an enhanced surface with a lower thermal conductivity, a higher actual temperature of heat transfer surface leads to a lower fin efficiency; this leads to poorer condensation heat transfer performance. Meanwhile, the area enhancement ratio of the HX tube is 1.44, which is greater than that of the 1EHT tube (1.34). Hence, the HX tube is more susceptible to thermal conductivity differences. Heat transfer enhancement of the HX tube made of copper is 1.13 to 1.18 times that of the SS tube for the same operating conditions; while enhancement ratio for the 1EHT tube is only 1.01 to 1.09. In conclusion, the tube thermal conductivity has a more significant effect on the HTC for the HX tube than on the 1EHT tube.

For mass flux values larger than 100 kg m^{-2} s^{-1}, the HTCs of all three tubes increase with an increase of the mass flux. However, for the enhanced tubes, the HTCs decrease with an increase of the mass flux when the refrigerant mass flux is less than 100 kg m^{-2} s^{-1}; at those values the main flow pattern is a stratified-wave flow; that is, the inner surface of the tube is divided into a submerged surface and unsubmerged surface. Gas-phase refrigerant transfers heat directly with the wall surface on the unsubmerged surface; this has a greater heat transfer efficiency. However, the latent heat released by the phase transition at the submerged surface can only reach the wall surface through the condensate by thermal conduction. As the mass flux increases, the shear force makes the condensate spread over the inner surface of the tube and causes a more serious inundation problem; the enhanced surface improves the function of surface tension and in turn intensifies the phenomenon; explaining why this trend appears only in the enhanced tubes and not in the smooth tube. Additional research is needed in this area to fully understand this.

Figure 4 presents the thermal resistance for in tube condensation heat transfer; for a mass flux of 200 kg $m^{-2}s^{-1}$. It can be seen that the thermal resistance ratios change with the thermal conductivity of the tube. Finally, only a slight variation occurs with the surface structure. Thermal conduction resistance of the wall is a small portion of the total resistance; the thermal resistance of the convection heat transfer on the refrigerant side dominates the process. The external surface of the 1EHT tube is enhanced, resulting in a lower outside thermal resistance; this is more evident in the SS tube. Total HTC of the 1EHT tube is the highest with both internal and external enhancement; it is followed by the HX tube and finally the smooth (ST) tube. Figure 5 shows the effect of tube diameter on the condensation HTC. For the most part, the HTCs of the 9.52-mm-OD tubes are higher than that of 12.7-mm-OD tubes. This can partially be explained by the fact that as the tube diameter decreases, the shear force and surface tension gradually take the place of gravity and they become the dominant forces; this is beneficial to removing and thinning the liquid film at the bottom. Additionally, the tube surface with a small diameter has a higher area density (ratio of surface area to volume); this leads to higher heat flux per unit volume. The trend of HTCs initially rising and then falling also appeared in the 9.52-mm-OD enhanced tubes; however, the turning point is delayed.

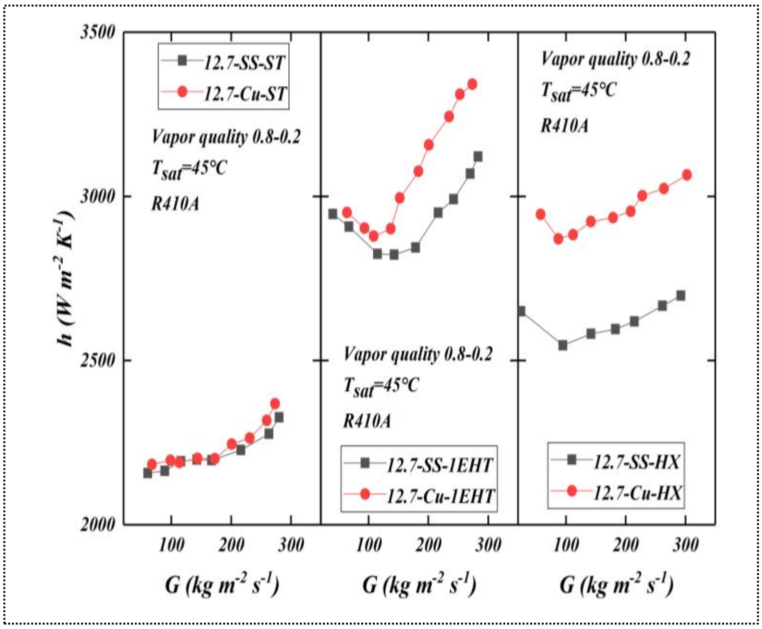

Figure 3: Comparison of condensation heat transfer coefficients inside 12.7-mm-OD copper and stainless steel tubes with various mass fluxes

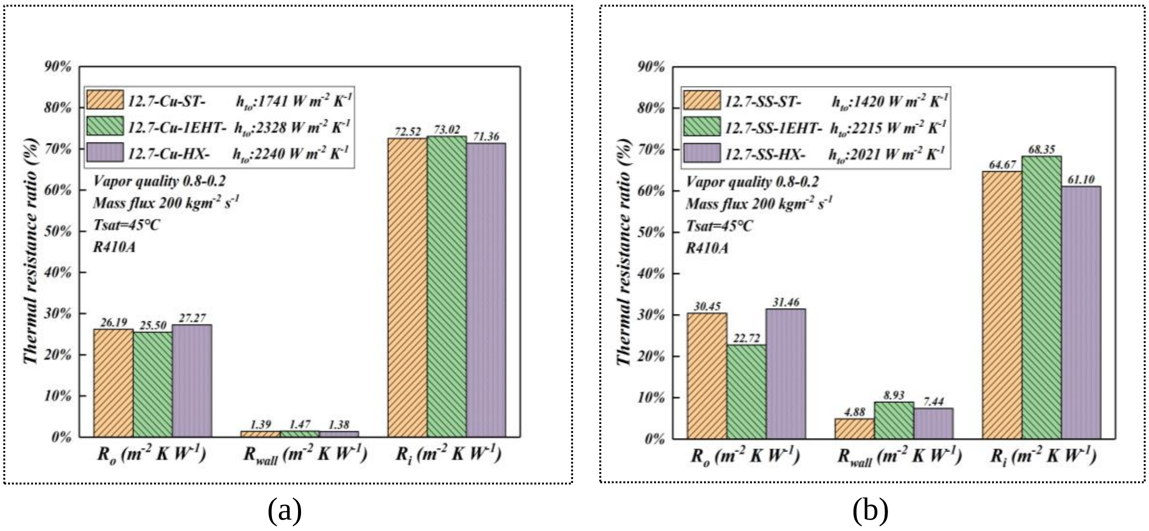

Figure 4: Comparison of the thermal resistance for (a) copper tubes and (b) stainless steel tubes

4. Conclusions

An experimental investigation of tubeside condensation heat transfer characteristics was performed using R410A in horizontal tubes that were enhanced and smooth. Effects of tube diameter and tube conductivity on the tubeside condensation heat transfer were discussed. The following conclusions can be drawn:

1. Smooth tube thermal-hydraulic performance is slightly affected by the thermal conductivity of the tube; however, the HTC of the enhanced tubes increase significantly with higher thermal conductivity tube material.

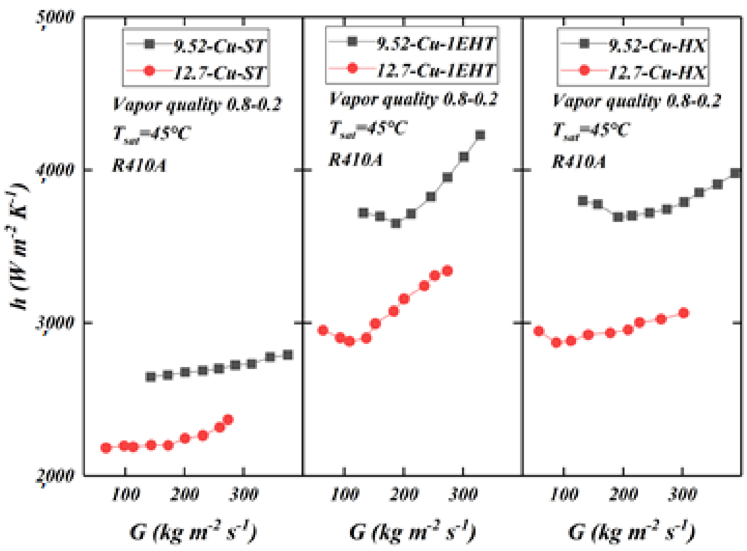

Figure 5: Condensation HTCs inside 9.52-mm-OD and 12.7-mm-OD copper tubes with various mass fluxes

2. Smaller tube diameters can achieve a better heat transfer performance; enhanced heat transfer is more obvious in the enhanced tubes.
3. It can also be concluded that tubes produced of higher thermal conductivity material or using a smaller diameter of the tube will lead to better heat transfer performance. They should be considered for high performance heat transfer systems.

References

Ali H.M., Briggs A., 2013, Condensation heat transfer on pin-fin tubes: Effect of thermal conductivity and pin height, Appl. Therm. Eng., 60, 465-471.

Gu Y., Liao Q., Cheng M., Ding Y., Zhu X., 2020, Condensation heat transfer characteristics of moist air outside a three-dimensional finned tube, Int. J. Heat Mass Transf., 158, 119983.

Ji W., Zhao C., Zhang D., Li Z., He Y., Tao W., 2014, Condensation of R134a outside single horizontal titanium, cupronickel (B10 and B30), stainless steel and copper tubes, Int. J. Heat Mass Transf., 77, 194–201.

Kukulka D.J., Smith R., Li W., 2014, Condensation and Evaporation Characteristics of Vipertex 1EHT Enhanced Heat Transfer Tubes, Chemical Engineering Transactions, 39, 727-732.

Kukulka D.J., Smith R., Li W., 2019, Experimental Comparison of the Evaporation and Condensation Heat Transfer Coefficients on the Outside of Enhanced Surface Tubes with Different Outer Diameters, Chemical Engineering Transactions, 76, 31-36.

Lemmon E. W., Huber M. L., Mclinden M. O., 2010, NIST Standard Reference Database 23: Reference Fluid Thermodynamic and Transport Properties-REFPROP. 9.0, NIST NSRDS.

Li G., Huang L., Tao L., 2017, Experimental investigation of refrigerant condensation heat transfer characteristics in the horizontal microfin tubes, Appl. Therm. Eng., 123, 1484–1493.

Li W., Tang W., Gu Z., Guo Y., Ma X., Minkowycz W.J., He Y., Kukulka D.J., 2020, Analysis of condensation and evaporation heat transfer inside 3-D enhanced tubes, Numerical Heat Transfer, Part A: Applications, 78 (10), 525-540.

Tang W., Sun Z., Li W., 2020, Visualization of flow patterns during condensation in dimpled surface tubes of different materials, Int. J. Heat Mass Transf., 161, 120251.

Zhang J., Zhou N., Li W., Luo Y., Li S., 2018, An experimental study of R410A condensation heat transfer and pressure drops characteristics in microfin and smooth tubes with 5 mm OD, Int. J. Heat Mass Transf., 125, 1284–1295.

Zhao C., Ji W., Jin P., Zhong Y., Tao W., 2017, The influence of surface structure and thermal conductivity of the tube on the condensation heat transfer of R134a and R404A over single horizontal enhanced tubes, Appl. Therm. Eng., 125, 1114–1122.